Available online at www.CivileJournal.org

Civil Engineering Journal

Vol. 4, No. 7, July, 2018

Structural Characteristics of Reinforced Palm Kernel Shell Concrete Deep Beams

Mark Adom-Asamoah [a*], Jack Banahene Osei [a] , Kwadwo Adinkra-Appiah [b]

[a] *Department of Civil Engineering, Kwame Nkrumah University of Science and Technology, Ghana.*

[b] *Department of Civil Engineering, Sunyani Technical University, Ghana.*

Received 29 May 2018; Accepted 03 July 2018

Abstract

This paper evaluates the structural characteristics of deep beams made from reinforced palm kernel shell concrete (PKSC) and normal weight concrete (NWC). Twelve PKSC and NWC deep beam samples, with and without shear reinforcement were tested under three-point loading and their structural behavior studied. The ultimate shear strength of PKSC beams increased with a decrease in the shear span-to- depth ratio. Post diagonal cracking shear resistance is greater in PKSC deep beams than beams of normal weight concrete. The shear capacity of the PKSC and NWC deep beams were assessed to be un-conservative using ACI 318-99, ACI 318-05, Euro code (EC) 2 and a kinematic model, when compared with the experimental results. Nonetheless, this necessitated the development of a calibration procedure to correct the bias inherent in these models. Calibrated shear strength models revealed the compressive strength and the ratio of the shear span-to-total depth as significant influential parameters for correcting the inherent bias in the original deterministic shear strength models. The calibrated functional model of ACI-318-99 may produce conservative predictions, given this limited number of test specimens. Therefore future studies should investigate the reliability of the calibrated models, and quantifying the uncertainties in the estimated coefficients of parameters, using a much larger representative dataset.

Keywords: Shear; Palm Kernel Shell; Deep Beams; Code Assessment.

1. Introduction

Concrete has a widespread application in the construction industry. The increased demand for concrete as a construction material, has yielded the investigation into unconventional building materials such as steel milled from scrap metals [1–3], bamboo reinforcement in concrete [4–6], phyllite aggregate waste in concrete [7], palm kernel shell aggregate in concrete [8, 9]. Conventionally, rocks of igneous, metamorphic and sedimentary origins such as granite, basalt, flint, limestone etc. [10, 11] have been used to produce coarse aggregates for concrete production over the years. Nonetheless, there has been increased use of coarse aggregates, which serve as economic filler in concrete, for construction purposes. This practice is leading to over-exploitation of natural rock resources in the environment and a depletion of sources of coarse aggregates.

There is therefore the need to find alternative coarse aggregate resources to replace natural ones. Research conducted on various solid waste materials; such as granulated coal ash, blast furnace slag, fiberglass waste materials, granulated plastics, sintered sludge pellets, phyllites from mining waste, ceramic waste and recycled concrete; as coarse aggregate substitutes has proved very successful [7, 12, 13]. Most of these waste materials constitute artificial light weight aggregates [14] and their introduction to replace conventional aggregates for concrete production in some developed

* Corresponding author: markadomasamoah@gmail.com

http://dx.doi.org/10.28991/cej-0309188

countries has been quite beneficial to the development of infrastructure [15]. Since the major characteristic properties of coarse aggregates impact directly on the resulting concrete properties such as compressive strength, shear strength, ductility behaviour and durability, it is important to evaluate the performance of alternative aggregate materials before accepted for general use. Palm Kernel Shell (PKS), a waste product from palm kernel oil production, is one such material that is receiving attention in recent times for use in the concrete industry due to its superior performance characteristics as coarse aggregate in lightweight concrete production [8].

One such use for PKS aggregate concrete is in the construction of RC beams. RC beams are classified into slender and deep beams [16]. Some previous studies conducted on PKSC slender beams have shown that it has satisfactory performance characteristics in compression, shear, flexure, ductility, aggregate interlock and bond with steel reinforcement [8, 14]. Hence, can be employed, especially in low-cost housing construction and also for use in earthquake prone areas due to its low weight advantage and ductility characteristics. On the other hand, RC beams where the shear span is less than twice the member depth are characterized by arch action rather than beam action, and are known as deep beams [17, 18]. More so, RC beams are known to exhibit low shear resistance when the depth of the beam increases [19, 20]. The conventional Euler-Bernoulli beam is usually not applicable to characterizing the shear behavior of such members, and as such, design concepts like strut and tie models, seems preferred. Recently, Tasenhod and Teerawong [21] developed an improved strut and tie model based on ACI 318-11. Kassem [22] adopted a fixed-angled softened truss model in the development of shear strength model for concrete deep beams, yielding reliable results than shear provisions as specified in the ACI code and Eurocode. Chou [23] presented a nature-inspired metaheuristic regression method for predicting shear strength of RC deep beams. It is worth noting that the developed shear strength models in these studies, employs a data set of conventional RC deep beams.

Virtually no research work has focused predicting the shear strength of PKSC deep beams. PKSC, as a light weight material for construction, could be a suitable material for the construction of RC deep beams as transfer girders in high-rise buildings designed to withstand seismic and other inertia forces due to their weight advantage and high ductility characteristics. The importance of the use of lightweight concrete in high-rise construction is highlighted by Metha and Monteiro [24], especially where the low bearing capacity of the soil was problematic. In one case, a lightweight concrete mix was used in the construction of a 52-storey building instead of 35-storey had it been a normal concrete building.

Deep beams usually fail through shearing action which tends to be more sudden and brittle [17, 25]. However, the accurate prediction of the shear strength of reinforced concrete deep beams is vital in engineering design and management [23]. Nonetheless, several of the developed shear strength models for RC deep beams either overestimate [21] or under estimate [26, 27] experimental observations. More so, studies that have evaluated the adequacy of code-based shear provisions have either reported relatively lower correlation coefficient [23] or larger coefficient of variation [26] in comparison with developed models. The adequacy of these models is highly reliant on the range of variables considered as well as the size of the database employed [28]. Hence it is becomes necessary to develop explicit shear strength model for PKSC deep beams. This study investigated the shear strength of 12 reinforced PKSC and Normal Concrete (NC) deep beams. The main variables considered in the study were shear span-to-effective depth ratio, vertical shear reinforcement ratio, and type of concrete. The shear capacity predictability of 3 codes of practice; ACI 318-99 (empirical formulae based), and ACI 318-05 and EC 2 (both based on strut-and-tie models) and one kinematic model were evaluated for such RC deep beams. A calibration procedure is proposed to provide reliable and consistent shear strength estimate for engineering design.

2. Materials and Method

According to Shetty [29], lightweight concrete mix design is usually established by trial mixes. Based on this method, a grade 30 concrete labeled as PKSC30 was designed, cast and tested for PKSC deep beams. Ordinary Portland cement of Grade 42.5 was used to achieve this target 28-day average compressive strength. The ratio of sand to cement and PKS to cement were 1.8 and 0.8 respectively based on a study conducted by [8]. Another concrete mix was produced from normal weight aggregate (granite) labelled NWC30 which was also designed with a target compressive strength of 30 MPa. Table 1 shows the mix proportions for the two types of concrete that were produced for analysis in the study.

Table 1. Mix proportion of concrete samples

Concrete mix Design	28-day Target Cube Strength (N/mm^2)	Cement Content (Kg/m^3)	Water/ Cement Ratio (W/C)	Sand/ Cement Ratio (S/C)	Coarse Aggregate/ Cement Ratio (A/C)	Super-Plasticizer (%)
PKSC30	30	450	0.40	1.8	0.7	1.5
NWC30	30	350	0.50	2.0	4.0	0.5

A total of 12 concrete beams, categorized into four groups were tested to ultimate failure. For each group the variable investigated is the shear span-to-depth ratio. Six concrete beams (Group 1 and 2) were without shear reinforcement. Group 1 and 3 were made of PKSC deep beams (see Table 2). Each group consist of three beams with clear spans of 500, 815 and 1125 mm, each with a constant cross section of 150 × 350 mm. All beams were designed to fail in shear.

Sufficient reinforcement anchorage was provided near the supports by providing a 150mm overhang beyond the support center lines to avoid premature anchorage failure. The beams were reinforced with 1.0% mild steel longitudinal reinforcement with yield strength of 413 MPa and elongation of 22% and cast in timber molds.

Six concrete cubes (150 ×150 ×150 mm) with six companion concrete modulus of rupture beams (100 × 100 × 500 mm) were cast, cured in water and tested after 28 days. The main variables considered in the study for the RC beams were shear span-to-effective depth ratio (a/d), vertical shear reinforcement ratio (ρ_v) and type of concrete (PKSC or NWC). Table 2 provides details of each concrete beams and Figure 1 shows a typical beam setup ready for testing. In Table 2, the beams are labelled first with the concrete type ('P' for PKSC or 'N' for NC), followed by the shear span-to-depth ratio (1.0, 1.5, 2.0) and vertical shear reinforcement (S0 for beams without vertical shear reinforcement and S1 for beams having shear reinforcement).

The loading and measuring system consisted of incrementally applying a monotonic load of 2 KN/min till ultimate failure is observed for test setup. An I-section steel spreader was place on top of each beam, and with the help of two roller supports, these monotonically increasing loads were transmitted, as schematically presented in Figure 1. The first flexural crack load, first diagonal cracking and ultimate failure were recorded along with their respective mid-span deflections measured with a dial gauge beneath the soffit of the beam under test. The maximum crack width and crack height were also taken, and crack patterns were marked on tested beams during loading.

Table 2. Test Matrix

	Beam	l_n (mm)	d (mm)	a/d	ρ_b (%)	ρ_v (%)	f_{cu} (MPa)
	P-1.0-S0	500	312	1.0	1.00	0.00	33.70
Group 1	P-1.5-S0	815	312	1.5	1.00	0.00	33.70
	P-2.0-S0	1125	312	2.0	1.00	0.00	33.70
	N-1.0-S0	500	312	1.0	1.00	0.00	42.93
Group 2	N-1.5-S0	815	312	1.5	1.00	0.00	42.93
	N-2.0-S0	1125	312	2.0	1.00	0.00	42.93
	P-1.0-S1	500	312	1.0	1.00	0.84	33.70
Group 3	P-1.5-S1	815	312	1.5	1.00	0.84	33.70
	P-2.0-S1	1125	312	2.0	1.00	0.84	33.70
	N-1.0-S1	500	312	1.0	1.00	0.84	42.93
Group 4	N-1.5-S1	815	312	1.5	1.00	0.84	42.93
	N-2.0-S1	1125	312	2.0	1.00	0.84	42.93

Where l_n is the clear span measured between edges of both support plates; d is the effective depth of the beam; a/d is the shear span to depth ratio; ρ_b is the longitudinal bottom reinforcement ratio; ρ_v is the vertical shear reinforcement ratio and f_{cu} is the cube compressive strength of concrete.

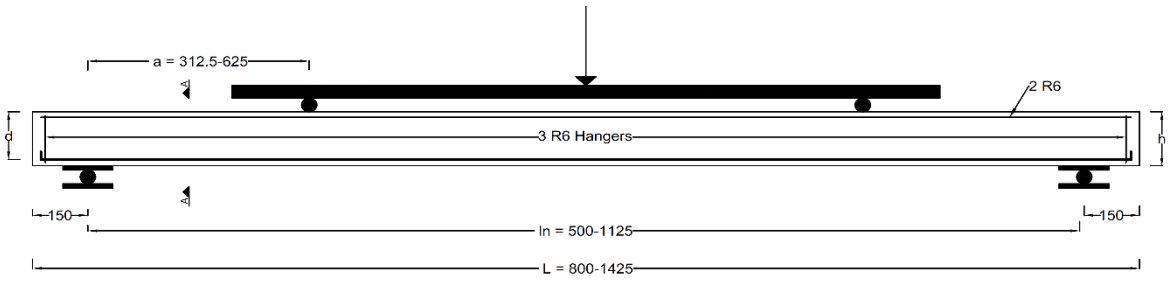

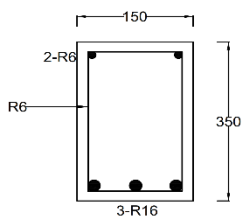

Section A-A

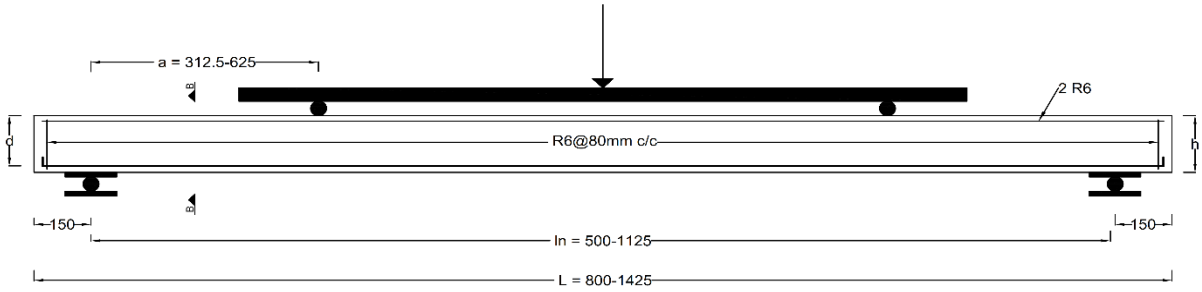

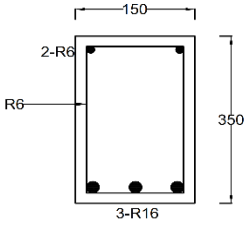

Section B-B

Figure 1. Experimental test setup

3. Test Results and Discussions

3.1. Mechanical Test on Aggregates, Pain Concrete Cubes and Plain Concrete Prisms

Laboratory test results for the coarse aggregates are given in Table 3 for both PKS and granite. The results indicate as reported by others [8, 30] that granite aggregates are superior to PKS in terms water absorption and density, which are parameters often linked to the durability and strength properties of concrete. The PKS however had a lower value of AIV compared to that of granite aggregates indicating that PKS aggregate concrete may possess a higher impact absorbance ability. The AIV is a measure of the relative resistance of aggregates to impact loads.

The 28-day compressive strength and modulus of rupture results were 33.70 and 1.19 MPa for the PKS and 42.93 and 2.88 MPa for the NWC samples respectively. The results of the concrete cube compressive strengths and those of the companion modulus of rupture beams are consistent with results from other researchers.

Table 3. Physical Properties of PKS and Granite Aggregates

Properties	PKS	Granite
Grain size (mm)	3 – 18	6.3 – 20
Shell thickness, mm	1 – 3	-
Specific gravity	1.02	2.75
Bulk unit weight, kg/m^3	588.75	917.50
24-Hour Water Absorption, %	6.75	0.68
Aggregate Impact Value, %	4.88	9.73

3.2. Load-Deflection and Structural Behavior

The load-deflection response of the PKSC and NC deep beams with and without shear reinforcement shows that as the a/d increased from 1.0 through 1.5 to 2.0, the failure load of the beams decrease (Figure 2).

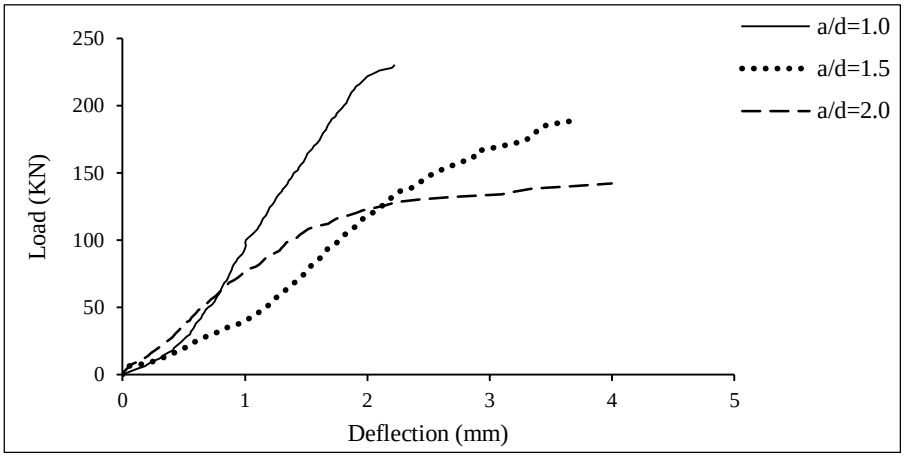

Figure 2. Typical load-deflection curve for PKSC deep beams without shear reinforcement

The PKSC deep beams experienced larger deflections in most cases at failure compared to the NC deep beams, particular for beam with vertical shear reinforcement (see Table 4). This conforms to findings of Alengaram et al. [8] that emphasizes that PKSC slender beams exhibit higher deflections at failure and hence possess higher ductility characteristics at failure than similar NWC slender beams. The deep beam samples without shear reinforcement failed by strut failure through diagonal-splitting, which signified the splitting of the concrete struts formed between the loading and the support points with a loud explosion at failure. The failure mode for beams without vertical shear reinforcements (Figure 3) was primarily diagonal tensile splitting of concrete struts, whereas those with vertical reinforcement failed in shear compression (Figure 4). These failure modes were independent on the type of concrete type. For instance, beams in Group 1 and 2 observed the same mode failure (see Table 4). In terms of crack patterns, flexural cracks appeared first around mid-span of the beams, as loading was applied, and these were followed by diagonal cracks, which emanated from the tip of the support plate at the bottom of the beam towards the loading plate on top of the beam for both PKSC and NC deep beam samples.

Table 4. Summary of test results

	Beam	f_{cu} (MPa)	P_{max} (KN)	$V_{cr,exp}$ (KN)	$V_{u,exp}$ (KN)	$V_{c,exp}/V_{u,exp}$ (%)	Crack width (mm)	Δ (mm)	v_{norm}	Failure mode
	P-1.0-S0	33.70	226	52	113	0.46	0.64	2.06	0.09	DS
Group 1	P-1.5-S0	33.70	190	42	95	0.44	1.60	3.73	0.07	DS
	P-2.0-S0	33.70	142	43	71	0.61	3.80	4.00	0.08	DS
	N-1.0-S0	42.93	224	81	112	0.72	0.50	2.10	0.05	DS
Group 2	N-1.5-S0	42.93	168	39	84	0.46	2.60	4.85	0.06	DS
	N-2.0-S0	42.93	164	54	82	0.66	1.78	2.95	0.05	DS
	P-1.0-S1	33.70	230	80	115	0.70	0.47	2.60	0.09	SC
Group 3	P-1.5-S1	33.70	226	47	113	0.42	1.30	4.04	0.07	SC
	P-2.0-S1	33.70	226	46	113	0.41	0.82	3.98	0.09	SC
	N-1.0-S1	42.93	230	105	115	0.91	0.45	2.28	0.07	SC
Group 4	N-1.5-S1	42.93	228	62	114	0.54	0.80	2.43	0.09	SC
	N-2.0-S1	42.93	224	59	112	0.53	0.62	2.97	0.07	SC

P_{max} is the maximum applied load; $V_{cr,exp}$ is the diagonal cracking shear; $V_{u,exp}$ is the ultimate shear; Δ is the mid-span deflection; v_{norm} is the normalized shear stress and is computed as $V_{u,exp}/(bdf_{cu})$; f_{cu} is the cylindrical compressive strength in MPa; DS is diagonal splitting; SC is shear compression.

Figure 3. PKSC deep beam without shear reinforcement

Figure 4. NWC deep beam with vertical shear reinforcement

Unlike the beams without shear reinforcement, the beams with vertical shear reinforcement experienced a more ductile failure with more number of cracks but less crack widths before failure (Figures 3 and 4). The PKSC deep beam samples experienced more number of cracks and wider crack widths at failure compared to the NC deep beams. Several flexural cracks appeared, as loading was increased until major diagonal strut cracks were observed between the loading plate and the support plates, which opened up gradually before failure occurred.

The shear strength of PKSC beams increased as a/d decreased (see Table 4). Nonetheless, the behavior of these beams after the formation of diagonal cracks is of prime importance. The parameter $V_{c,exp}/V_{u,exp}$ is used herein to assess the extra load sustained after the initiation of the first diagonal crack ($V_{c,exp}$) to the ultimate failure ($V_{u,exp}$). The increase in shear strength above the diagonal cracking load ranged between 10 to 140 %.The post-diagonal cracking shear resistance is greater in PKS than NC beams ($V_{c,exp}/V_{u,exp}$), irrespective of the presence of transverse reinforcement (on average14%) (see Table 4). For beams without vertical shear reinforcement, loads of about twice the diagonal crack load can be sustained before ultimate failure ($V_{c,exp}/V_{u,exp}$ of Table 4), on the average. It is also expected that the ultimate shear strength resistance for PKS is higher than Normal Concrete. Nonetheless, the contribution of transverse reinforcement to shear resistance may be slightly high in NC deep beams than PKSC deep beams at a particular level.

Comparison of the shear capacities of the PKSC and NWC deep beams can be better achieved by normalizing the ultimate shear load by its corresponding 28-day cube compressive strength of the concrete (v_{norm}). The results indicates that PKSC deep beams exhibit higher normalized shear strength characteristics compared to the NWC deep beams (see Table 4). This confirms the result of Alengaram et al. [8] which reported higher shear strength for PKSC slender beams compared to the control NC beams.

4. Shear Strength Models of Deep Beams

The traditional sectional design approach which applies the Bernoulli's assumptions of linear strain variation of a beam section and also assumes a parallel chord truss model is not applicable to deep beams. This is because, as a result of the small a/d ratios in a deep beam (a/d<2.5), a large portion of the loads is transferred directly to the supports via compression struts forming a tied-arch. Shear design of deep beams employed by several codes of practice may be classified into two major categories; those that use empirical formulae and those based on the analytical strut-and-tie models. Nonetheless, Mihaylov et al. [31] recently proposed a kinematic model for estimating the shear strength of deep beams by quantifying the individual contributions from aggregate interlock, dowel actions and stirrups. The shear transfer capabilities of a typical empirical formulae code (ACI 318-99 [32]), those of 2 strut-and-tie models (ACI 318-

05 [33] and EC 2 [34]), and a kinematic model of Mihaylov et al. [31] are compared with experimental data obtained for PKSC and NC beams. These 4 codes of practice have been chosen as samples representing the two categories, as well as recently developed approach, in order to assess the validity of both categories in estimating the shear capacity of PKSC deep beams with and without vertical reinforcement. The main features of shear provisions of deep beams in the four design codes are presented below.

ACI 318-99

The nominal shear capacity V_n of deep beams is proposed as follows

$$V_n = V_c + V_s \quad (1)$$

$$V_c = \left(3.5 - 2.5\frac{M_u}{V_u d}\right)\left(0.16\sqrt{f_c'} + 17\rho_b\frac{V_u}{M_u}\right)b_w d \leq \quad 0.5\sqrt{f_c'}b_w d \quad (2)$$

$$V_s = \left[\rho_v\left(\frac{1 + {l_n}/{d}}{12}\right) + \rho_h\left(\frac{11 - {l_n}/{d}}{12}\right)\right]b_w d f_y \quad (3)$$

Where V_c and V_s are the transfer capacities of concrete and shear reinforcement respectively; M_u and V_u are factored moment and shear force at the critical section, respectively; b_w is section width; d is the effective depth of section; l_n is the clear span measured between edges of both support plates; f_c' is concrete compressive strength; $\rho_b = A_s/b_w d$ is the longitudinal bottom reinforcement ratio; A_s is the area of longitudinal bottom reinforcement; $\rho_v = A_v/b_w s_v$ is the vertical reinforcement ratio; A_v and s_v are the area and spacing of vertical shear reinforcement respectively; $\rho_h = A_h/b_w s_h$ is the horizontal shear reinforcement ration; A_h and s_h are the area and spacing of horizontal shear reinforcement respectively; f_y and is the yield strength of shear reinforcement.

Depending on l_n/d , shear capacity calculated from equation (1) is limited by the following expressions

$$V_n \leq 0.67\sqrt{f_c'}b_w d \text{ for } l_n/d \leq 2 \quad (4a)$$

$$V_n \leq \frac{1}{18}\left(10 + \frac{l_n}{d}\right)\sqrt{f_c'}b_w d \text{ for } 2 \leq l_n/d \leq 5 \quad (4b)$$

For simple deep beams

$$\frac{M_u}{V_u d} = \frac{a}{2d} \quad (5)$$

Where a is the shear span.

ACI 318-05

The shear capacity of simple beams V_n owing to failure of concrete struts is

$$V_n = F_E \sin\theta \quad (6)$$

Where F_E is the load capacity of concrete struts and θ is the angle between the concrete strut and the longitudinal axis of deep beam, which is expressed as $\tan^{-1}(jd/a)$ and shall not be less than 25°. The distance between the centre of top and bottom nodes jd, in simple deep beams is given by

$$jd = h - c - w_t^i/2 \quad (7)$$

Where c the cover of is longitudinal bottom reinforcement, h is the overall depth of section and w_t' is the depth of the top node. The depth of the bottom node w_t is approximately assumed to be

$$w_t = 2c \quad (8)$$

The depth of the top node can be calculated by

$$w_t' = 1.25 w_t \quad (9)$$

The average effective widths $(w_s)_E$ of concrete struts uniformly tapered in shear can be calculated from

$$(w_s)_E = \frac{2.25 w_t \cos\theta + [(l_p)_E + (l_p)_p]\sin\theta}{2} \quad (10)$$

Where $(l_p)_P$ and $(l_p)_E$ are the widths of loading and end support plates respectively.

The load capacity of a simply supported deep beam is

$$F_E = v_e f'_c b_w (w_s)_E \quad (11)$$

Where v_e is the effectiveness factor of concrete taking as 0.75.

The minimum amount of shear reinforcement required in bottle-shaped struts which is recommended to be placed in two orthogonal directions is suggested by ACI 318-05 as follows

$$\sum \frac{A_{si}}{b_w S_i} \sin\gamma_1 \geq 0.003 \quad (12)$$

Where A_{si} and s_i are the total area and spacing of the ith layer of reinforcement crossing a strut respectively and γ_i is the angle between the ith layer of reinforcement and a strut. The value of the effectiveness factor drops to 0.6 if the minimum shear reinforcement defined in equation (12) above is not provided.

EC2

The equations for EC2 are similar to those of ACI 318-05. The effectiveness factor of concrete, dependent only on concrete compressive strength and does not consider the effect of shear reinforcement and transverse tensile strain, is stipulated as follows

$$v_e = 0.61(1 - f'_c/250) \quad (13)$$

The top node depth is given by

$$w_t = 1.176 w_t \quad (14)$$

According to EC 2 the shear resistance due to vertical shear reinforcements is given by the lesser of

$$V_{Rd,s} = \frac{A_{sw}}{s} z f_{ywd} \cot\theta \quad (15)$$

$$V_{Rd,max} = \alpha_{cw} b_w z v_e f_{cd} / (\cot\theta + \tan\theta) \quad (16)$$

Where A_{sw} is the cross-sectional area of the shear reinforcement, s is the spacing of the stirrups, f_{ywd} is the design yield strength of the shear reinforcement, α_{cw} is a coefficient taking account of the state of the stress in the compression chord (taken as 1), z is given by 0.9d.

Kinematic Model

For the calculation of the shear strength of deep beams using the kinematic model V_{KM}, Mihaylov et al. (2013) used the following equation:

$$V_{KM} = V_{ci} + V_{CLZ} + V_s + V_d \quad (17)$$

Where V_{ci}, V_{CLZ}, V_s and V_d are the shear forces resisted by aggregate interlock, by the critical loading zone, by stirrups, and by dowel action, respectively.

The aggregate interlock shear component V_{ci} is expressed as follows:

$$V_{ci} = \frac{0.18\sqrt{f'_c}}{0.31 + \frac{24w}{a_{ge}+16}} bd \quad (18)$$

Where a_{ge} is the effective aggregate size which equals the coarse aggregate maximum size a_g for concrete strengths less than 60 MPa and zero for strengths larger than 70 MPa, with a linear transition for intermediate strengths. The crack width w is calculated according to the following:

$$w = \Delta_c \cos\alpha_0 \quad (19)$$

Where α_o is the angle of the critical crack to the longitudinal axis of the beam at shear failure and it can be evaluated as:

$$\tan\alpha_0 = \frac{d}{s_{max} + 1.5l_{be}} \quad (20)$$

The vertical displacement Δ_c of the critical loading zone is calculated using the following equation:

$$\Delta_c = 0.0150 l_{be} \cot\alpha \quad (21)$$

Where l_{be} is the effective width of the loading plate and should not be taken less than three times the maximum size of coarse aggregate, a_g; α is the angle of line extending from inner edge of support plate to far edge of tributary area of loading plate. The term s_{max} is the spacing of the radial cracks at the bottom of the section which can be calculated as follows:

$$s_{max} = \frac{0.28 d_b}{\rho_1} \frac{2.5(h - d)}{d} \quad (22)$$

Where d_b is the bar diameter, h is the beam total depth, and ρ_1 is the ratio of bottom longitudinal reinforcement.

The shear strength of the critical loading zone V_{CLZ} is calculated from:

$$V_{CLZ} = k_{11} f_{avg} b l_{be} \sin^2\alpha \quad (23)$$

Where k_1 is a crack shape coefficient which can be taken as 1 for beams with $\cot\alpha \leq 2.5$ and zero for beams with $\cot\alpha \geq 2.5$, with a linear transition for intermediate values of $\cot\alpha$. The average compressive stress f_{avg} in the critical loading zone can be calculated as follows:

$$f_{avg=} 1.43 f_c'^{0.8} \quad (24)$$

The shear component resisted by the stirrups V_s is expressed as follows:

$$V_s \rho_w b(d\cot\alpha - l_0 - 1.5l_{be}) f_w \geq 0 \quad (25)$$

Where ρ_w is the ratio of stirrup reinforcement, f_w is the stress in the stirrups. Quantity l_o is the length of the heavily cracked zone at the bottom of the critical crack and is determined as follows:

$$l_0 = 1.5(h - d)\cot\alpha \geq s_{max} \quad (26)$$

The stress in the stirrups is calculates as:

$$f_w = E_s \varepsilon_v \leq f_{yw} \quad (27)$$

Where f_{yw} is the yield strength of the stirrups and the stirrup strain ε_w is calculated as:

$$\varepsilon_w = \frac{1.5\Delta_c}{0.9d} \quad (28)$$

The shear component resisted by the dowel action of the bottom reinforcement is calculated from:

$$V_d = n_b f_{ye} \frac{d_b^3}{3l_k} \quad (29)$$

Where n_b is the number of bars, f_{ye} is the effective yield strength of the bars and can be taken as the yield strength of the bars f_y and not be taken more than 500 MPa. At shear failure, the dowel length l_k can be taken as l_o given in equation 26.

4.1. Assessment of Shear Models

Table 5 presents results of the predicted shear strength of the tested beams for the four shear models outlined above. Generally, predictions were higher in relation to the true experimental strength observed after testing. In other words, the four models overestimated the shear strength and can be seen to be un-conservative for design. This phenomenon was assessed by employing the ratio between the experimental shear failure load ($V_{u,exp}$) to the estimated shear capacity (V_{pred}) computed from these models. Summary statistics as presented in Table 5 shows that ACI-318-99 [32] may perform better than the other models (average $V_{u,exp}/ V_{pred}$ of 0.74). EC2 [34] can be seen as the worst predictive model, and highly un-conservative. This necessitates the development of a calibration procedure to better assess the performance of these models for predicting shear strength of PKSC deep beams.

Table 5. Assessment of Shear Strength Model

Beam	$V_{u,exp}$ (KN)	ACI-318-99		ACI-318-05		EC2		Kinematic Model	
		V_{STM} (KN)	$V_{u,exp}/ V_{pred}$	V_{STM} (KN)	$V_{u,exp}/ V_{Spred}$	V_{STM} (KN)	$V_{u,exp}/ V_{pred}$	V_{STM} (KN)	$V_{u,exp}/ V_{pred}$
P-1.0-S0	113	103.3	1.09	218	0.52	195.3	0.58	221.4	0.51
P-1.5-S0	95	103.3	0.92	153.4	0.62	137.7	0.69	149.7	0.63
P-2.0-S0	71	103.3	0.69	113.3	0.63	101.8	0.7	106.9	0.66
N-1.0-S0	112	137.1	0.82	277.7	0.4	240.6	0.47	261.8	0.43
N-1.5-S0	84	137.1	0.61	195.4	0.43	169.6	0.5	175.9	0.48
N-2.0-S0	82	132.5	0.62	144.3	0.57	125.3	0.65	124.6	0.66
P-1.0-S1	115	138.4	0.83	272.4	0.42	349.3	0.33	221.4	0.52
P-1.5-S1	113	144.7	0.78	191.7	0.59	369.3	0.31	149.7	0.75
P-2.0-S1	113	156.1	0.72	141.6	0.8	336.7	0.34	106.9	1.06
N-1.0-S1	115	183.8	0.63	347.1	0.33	394.6	0.29	261.8	0.44
N-1.5-S1	114	192.2	0.59	244.2	0.47	401.2	0.28	175.9	0.65
N-2.0-S1	112	207.3	0.54	180.3	0.62	414.7	0.27	124.6	0.9
Mean			0.74		0.53		0.45		0.64
SD			0.16		0.13		0.17		0.19
COV(%)			22		24		37		30

4.2. Calibration of Shear Models

Section 4.1 presented results indicating that the selected basic shear models produce shear capacities higher than experimental values, and as such it is imperative to correct the bias inherent in these models. The calibration procedure adopted herein involves multiplying the original estimated shear strength values (V_{pred}) by a factor (ξ) which is function of most of the major shear influential parameters. Mathematically

$$V_{cal} = V_{pred}\xi(\Theta) \tag{30}$$

Where V_{cal} is the shear capacity after calibration, V_{pred} is the original shear estimates for each shear model and $\xi(\Theta)$ is the correction factor which is a function of some of the parameters that influences shear strength. The selected parameters, Θ, are a/d, f_{cu}, l_n/d, c, ρ_b and ρ_v. A forward stepwise regression was conducted in the log-transformed space of these parameters/predictors (Θ) on the ratio $V_{u,exp}/V_{pred}$, assuming that the calibrated response (V_{cal}) will be equal to the experimental response ($V_{u,exp}$). Forward stepwise was selected because of the fairly lower number of beams investigated in comparison to the number of predictors, and also to identify the predictors that are significant. A typical calibrated model could be mathematically represented as

$$V_{cal} = e^{\beta_o} V_{pred} \prod_{i=1}^{p} \theta_i^{\beta_i} \tag{31}$$

Where β_o and β_is are estimated intercept and coefficients of the parameters in the regression analysis, and p is the number of significant parameters retained after regression. These estimates are given in Table 6.

Table 6. Models parameters after Calibration

Parameter	Estimated Coefficients			
	ACI-318-99	ACI-318-05	EC-2	Kinematic Model
Intercept	-0.059	2.568	-16.684	7.451
a/d	-	-	-	-
f_{cu}	-1.140	-0.992	-0.707	-0.657
l_n/d	-	-	-	-
a/h	-0.370	0.643	0.164	0.758
d/h	-	-	-	-
ρ_b	-	-	-	-
ρ_v	-0.763	-	-3.734	1.208
RMSE (before)	40.63	114.19	194.11	80.99
RMSE (after)	48.34	17.56	20.55	17.37
ABS (before)	33.75	93.60	158.55	62.41
ABS (after)	13.64	15.05	15.17	14.88

Results indicates that the compressive strength, f_{cu}, and the ratio of the shear span to the overall height (a/h) as significant contributors for bias-correction, considering the selected shear strength models (Table 6). More so, ACI-318-99 produced the lowest absolute error (ABS) after bias-correction, with the kinematic model producing the least value of the root mean-squared error (RMSE), also after bias-correction. The calibrated shear models are assessed on the tested beams and presented in Table 7. Generally, the means of the ratio of the shear experimental shear failure load ($V_{u,exp}$) to the calibrated shear capacity (V_{cal}) were 1.0 for all the shear models except ACI 318-99 (1.02). Hence, employing the calibrated shear model of ACI 318-99 can yield conservative estimates compared to the others, particularly for design purposes. In order to better understand and determine which of the models is appropriate for design, Figure 5 shows the predicted shear against the experimental observed responses for the four shear strength models. The dotted line is used to demarcate the boundary for which the predicted response may be either above or below the experimental responses. Observations above the dotted line produces conservative estimates (predicted shear strength lesser than experimental response). A critical assessment reveals that only 3, 6, 6 and 5 of the beams had calibrated responses greater than the experimental (un-conservative) for the ACI 318-99, ACI-318-05, EC2 and Kinematic Model respectively. This suggests that the developed calibrated model of ACI-318-99 can be fairly used to quantify the shear strength of PKS deep beams during structural design. Nevertheless, it yields predictions with the lowest scatter (coefficient of variation) among the four calibrated models presented.

Table 7. Assessment of Calibrated Shear Models

Beam	$V_{u,exp}$ (KN)	ACI-318-99		ACI-318-05		EC2		Kinematic Model	
		V_{cal} (KN)	$V_{u,exp}/V_{cal}$	V_{cal} (KN)	$V_{u,exp}/V_{cal}$	V_{cal} (KN)	$V_{u,exp}/V_{cal}$	V_{cal} (KN)	$V_{u,exp}/V_{cal}$
P-1.0-S0	113	150.0	1.08	100.7	1.12	118.1	0.96	100.5	1.12
P-1.5-S0	95	90.3	1.05	92.1	1.03	89.0	1.07	92.6	1.03
P-2.0-S0	71	81.3	0.87	81.7	0.87	68.9	1.03	82.1	0.86
N-1.0-S0	112	105.8	1.06	100.9	1.11	122.6	0.91	101.4	1.10
N-1.5-S0	84	91.0	0.92	92.3	0.91	92.4	0.91	92.9	0.90
N-2.0-S0	82	79.2	1.04	81.8	1.00	71.6	1.15	81.6	1.00
P-1.0-S1	115	121.3	0.95	125.8	0.91	108.1	1.06	124.8	0.92
P-1.5-S1	113	110.4	1.02	115.1	0.98	122.2	0.92	115.0	0.98
P-2.0-S1	113	107.2	1.05	102.1	1.11	116.8	0.97	102.0	1.11
N-1.0-S1	115	114.9	1.00	126.1	0.91	102.9	1.12	126.0	0.91
N-1.5-S1	114	106.3	1.07	115.3	0.99	111.9	1.02	115.3	0.99
N-2.0-S1	112	100.0	1.12	102.3	1.09	121.2	0.92	101.4	1.10
Mean			1.02		1.00		1.00		1.00
SD			0.07		0.09		0.08		0.09
COV(%)			7		9		8		9

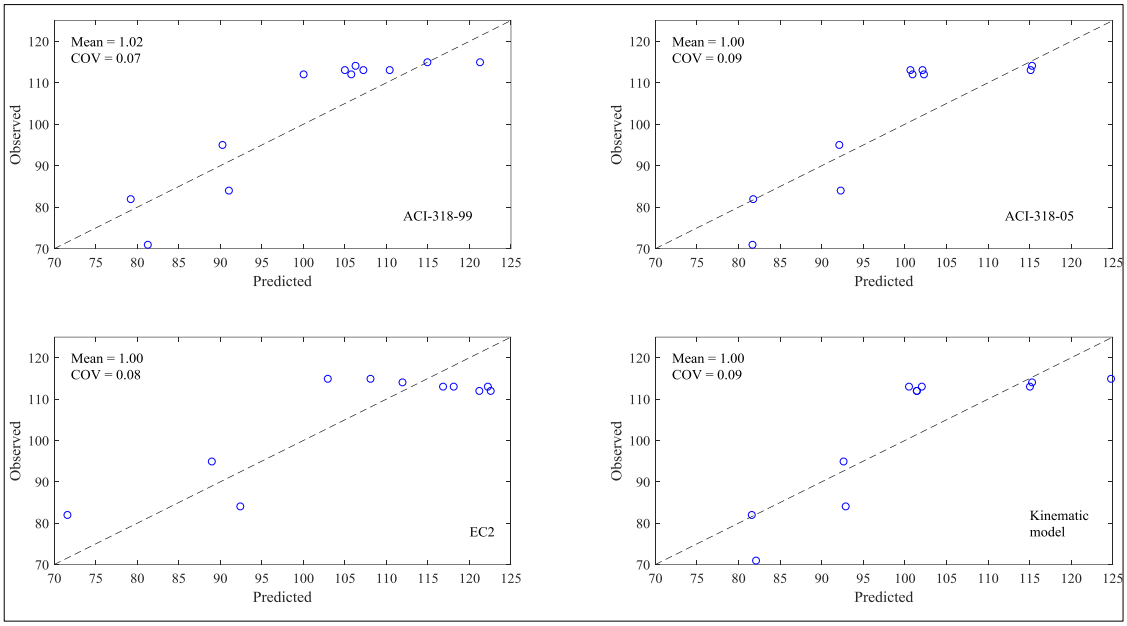

Figure 5. Assessment of Calibrated Shear Strength Models

5. Conclusion

The shear behavior of reinforced palm kernel shell concrete deep beams is investigated. 12 test specimen were subjected to a three-point bending test to ultimate failure. The concrete type (Palm Kernel Shell (PKS) Concrete and Normal Concrete), the shear-span to depth ratio (a/d) and the vertical reinforcement ratio (ρ_v) were the major variables investigated. Four shear strength models for deep beams as documented in ACI 318-99, ACI-318-05, EC2 and a recently proposed kinematic model were used to assess their predictability in relation to PKS deep beams. The major findings are:

- The ultimate shear strength of PKSC beams increased with a decrease in the shear span-to- depth ratio. More so, post diagonal cracking shear resistance is greater in PKSC deep beams than beams of normal concrete. The expected improvement in post-diagonal cracking resistance of such beams averages to about 14%.
- Design shear provisions documented in ACI-318-99, ACI-318-05, EC 2, as well as the Kinematic model of Mihaylov et al. (2013) yielded un-conservative predictions for the investigated deep beams. Among these basic shear strength model, ACI-318-99 performed better than the other models. This necessitates the development of a calibration procedure to better assess the performance of these models at predicting the shear strength PKSC beams. Calibrated shear strength models revealed the compressive strength and the ratio of the shear span-to-total depth as significant influential parameters for correcting the inherent bias in the original deterministic shear strength models. The calibrated functional model of ACI-318-99 may produce conservative predictions, given this limited number of test specimens. Therefore future studies should investigate the reliability of the calibrated models, and quantifying the uncertainties in the estimated coefficients of parameters, using a much larger representative dataset.

6. References

[1] Adom-Asamoah M, Kankam CK. Behaviour of reinforced concrete two-way slabs using steel bars milled from scrap metals. Mater Des 2008;29:1125–1130.

[2] Adom-Asamoah M, Kankam CK. Flexural behaviour of one-way concrete slabs reinforced with steel bars milled from scrap metals. Mater Des 2009;30:1737–1742.

[3] Subasi S, Cullu M. Investigating of adequacy of steel bars, produced from iron ore and scraped steel for concrete. J Fac Eng Arch Gazi Univ 2006;21:612–29.

[4]Adom-Asamoah M, Osei JB. Shear Performance of Bamboo Reinforced Self- Compacting Concrete Beams Without Stirrups. ARPN J Eng Appl Sci 2018;13:3312–24.

[5] Adom-Asamoah M, Osei J, Afrifa R. Bamboo reinforced self-compacting concrete one-way slabs for sustainable construction in rural areas. Cogent Eng 2018;5:1–13. doi:10.1080/23311916.2018.1477464.

[6] Ghavami K. Bamboo as reinforcement in structural concrete elements. Cem Concr Compos 2005;27:637–49.

[7] Adom-Asamoah M, Afrifa RO. Shear behaviour of reinforced phyllite concrete beams. Mater Des 2013;43:438–446.

[8] Alengaram U., Jumaat MZ, Mahmud H. Ductility behaviour of reinforced palm kernel shell concrete beams. Eur J Sci Res 2008;23:406–20.

[9] Acheampong A, Adom-Asamoah M, Ayarkwa J, Afrifa RO. Code Compliant Behaviour of Palm Kernel Shell Reinforced Concrete (RC) Beams in Shear. J Civ Engineeing Constr Technol 2015;6:59–70.

[10] Bhatt P, Macginley TJ, Choo BS. Reinforced Concrete: Design Theory and Examples. Taylor & Francis; 2006.

[11] BS812. Specification of Aggregates for Concrete, Part 1 1975.

[12] Emmitt S. Barry's Introduction to Construction of Buildings. John Wiley & Sons; 2010.

[13] Moulinier F, Lane S, Dunster A. The use of glass as aggregate in in Portland cement concrete. Waste Resour. Action Programme WRAP, Banbury, Oxon: 2006.

[14] Teo DC., Mannan MA, Kurian VJ, Zakaria I. Flexural behaviour of reinforced lightweight OPS concrete beams, Malaysia: 2006, p. 244–252.

[15] Mahmud HB, Majuar E, Zain MFM, Hamid NB a. A. Mechanical Properties and Durability of High Strength Concrete Containing Rice Husk Ash. Spec Publ 2004;221:751–66. doi:10.14359/13289.

[16] Rogowsky DM, MacGregor JG, Ong SY. Tests of Reinforced Concrete Deep Beams. Edmonton: University of Alberta; 1983.

[17] ACI 318. Building Code Requirements for Structural Concrete (ACI 318-08) and Commentary 2008.

[18] Shuraim AB. Behavior and shear design provisions of reinforced concrete D-region beams. J King Saud Univ - Eng Sci 2013;25:65–74. doi:10.1016/j.jksues.2012.01.001.

[19] Dahake A. Flexural analysis of deep beam subjected to parabolic load using refined shear deformation theory. Appl Comput Mech 2012;6:163–72.

[20] Appa Rao G, Sundaresan R. Size Dependent Shear Strength Of Reinforced Concrete Deep Beams Based On Refined Strut-And-Tie Model. J Front Constr Eng 2014;3:9–19.

[21] Tasenhod P, Teerawong J. Shear Strength Prediction of Reinforced Concrete Deep Beams Using Strut-and-Tie Model. Adv Mater Res 2014;931–932:468–72. doi:10.4028/www.scientific.net/AMR.931-932.468.

[22] Kassem W. Shear strength of deep beams: a mathematical model and design formula. Struct Concr 2015;16:184–94. doi:10.1002/suco.201400045.

[23]Chou J-S, Ngo N-T, Pham A-D. Shear Strength Prediction in Reinforced Concrete Deep Beams Using Nature-Inspired Metaheuristic Support Vector Regression. J Comput Civ Eng 2016;30:04015002.

[24] Monteiro P. Concrete: microstructure, properties, and materials. McGraw-Hill Publishing; 2006.

[25] Appa Rao G, Kunal K. Shear strength of Reinforced Concrete deep beams, Catania, Italy: 2007, p. 671–5.

[26] El-Sayed AK, Shuraim AB. Size effect on shear resistance of high strength concrete deep beams. Mater Struct 2016;49:1871–82. doi:10.1617/s11527-015-0619-1.

[27] El-Zoughiby ME, El-Metwally SE, Al-Shora AT, Agieb EE. Strength Prediction of Simply Supported R/C Deep Beams Using the Strut-and-Tie Method. Arab J Sci Eng 2013;38:1973–91. doi:10.1007/s13369-013-0609-y.

[28] liu J, Mihaylov B. A comparative study of models for shear strength of reinforced concrete deep beams. Eng Struct 2016;112:81–9.

[29] Shetty MS. Concrete technology theory and practice. 2005.

[30] Ching D, Teo L, Kurian VJ. Production of lightweight concrete using oil palm shell (OPS) aggregates 2018.

[31] Mihaylov BI, Bentz EC, Collins MP. Two-Parameter Kinematic Theory for Shear Behavior of Deep Beams. Struct J 2013;110:447–56. doi:10.14359/51685602.

[32] American Concrete Institute. Building Code Requirements for Structural Concrete (318-99) and Commentary—(318R-99). 1999.

[33] American Concrete Institute. Building Code Requirements for Structural Concrete (ACI 318-05) and Commentary (ACI 318R-05). 2005.

[34] British Standards Institution. The European Standard EN 1992-1-1:2004. Eurocode 2: Design of concrete structures. 2004.